

Elliptic flow of J/ψ at forward rapidity in Pb-Pb collisions at 2.76 TeV with the ALICE experiment

Hongyan Yang (for the ALICE Collaboration)¹

SPhN/Irfu, CEA-Saclay, Orme des Merisier, 91191 Gif-sur-Yvette, France

Abstract

We present the elliptic flow of inclusive J/ψ measured in the $\mu^+\mu^-$ channel at forward rapidity ($2.5 < y < 4.0$), down to zero transverse momentum, in Pb-Pb collisions at $\sqrt{s_{NN}} = 2.76$ TeV with the ALICE muon spectrometer. The p_T dependence of J/ψ v_2 in non-central (20%-60%) Pb-Pb collisions at $\sqrt{s_{NN}} = 2.76$ TeV is compared with existing measurements at RHIC and theoretical calculations. The centrality dependence of the p_T -integrated elliptic flow, as well as the p_T dependence in several finer centrality classes is presented.

1. Introduction

Charmonium production in heavy ion collisions has been studied at different energies and with different collision systems, ever since the J/ψ suppression induced by color screening of its constituent quarks was proposed as a signature of the formation of a quark gluon plasma (QGP) in heavy-ion collisions [1]. The recent measurement of the J/ψ production in Pb-Pb collisions at forward rapidity performed by ALICE at the LHC [2] clearly showed less suppression compared with SPS and RHIC results [3, 4]. At RHIC energies, the preliminary result from the STAR collaboration showed a J/ψ elliptic flow in Au-Au collisions at $\sqrt{s_{NN}} = 200$ GeV [5] consistent with zero within uncertainties in the measured p_T range (0-10 GeV/c). A non-zero measurement of quarkonium elliptic flow is especially promising at the Large Hadron Collider (LHC) where the high energy density of the medium and the large number of $c\bar{c}$ pairs produced in Pb-Pb collisions is expected to favor the flow development and regeneration scenarios.

2. Data analysis and results

The ALICE detector is described in [6]. At forward rapidity ($2.5 < y < 4.0$) the production of quarkonium states is measured in the muon spectrometer down to $p_T = 0$. The data sample used for this analysis corresponds to 17 M dimuon unlike sign (MU) triggered Pb-Pb collisions collected in 2011. It corresponds to an integrated luminosity $L_{int} \approx 70 \mu\text{b}^{-1}$. The event and muon track selection are the same as described in [7], except for an additional requirement of the event vertex position $|Z_{vtx}| < 10$ cm to ensure a flat event plane distribution. J/ψ candidates are formed by combining pairs of opposite-sign (OS) tracks reconstructed in the geometrical acceptance of the muon spectrometer.

¹A list of members of the ALICE Collaboration and acknowledgements can be found at the end of this issue.

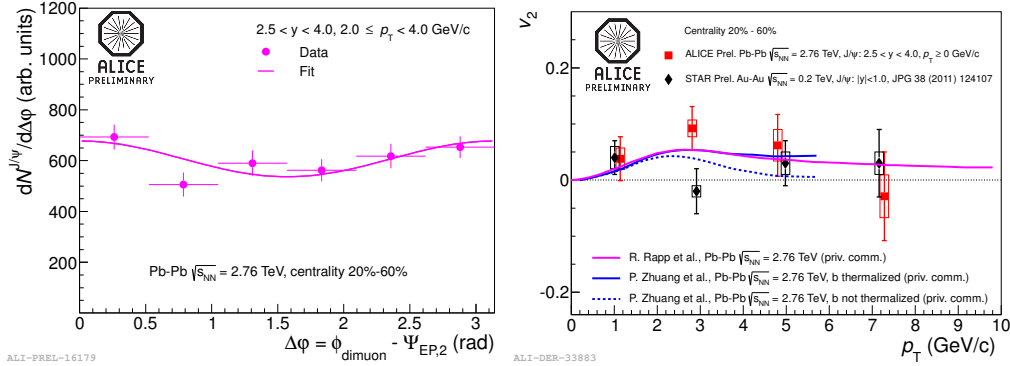


Figure 1: Left: v_2 extraction with the event plane method in which the J/ψ raw yield is plotted as a function of $\Delta\varphi$ using a fit to the data with $dN^{J/\psi}/d\Delta\varphi = A \times (1 + 2v_2^{\text{obs}} \cos 2\Delta\varphi)$. Right: Inclusive J/ψ v_2 in the centrality bin 20%-60% as a function of p_T . A comparison to STAR results and to two parton transport model calculations [10, 11] are shown. The vertical bars show the statistical uncertainties, and the boxes indicate the point-to-point uncorrelated systematic uncertainties, which are dominated by the signal extraction.

22 The J/ψ v_2 is measured using event plane based methods [8]. To make a direct comparison
 23 with lower energy measurements, the inclusive J/ψ v_2 (p_T) was calculated in the same centrality
 24 range 20%-60% as at RHIC [5], as discussed in detail in [9]. The v_2 is extracted by fitting the J/ψ
 25 raw yield as a function of $\Delta\varphi = \phi_{\text{dimuon}} - \Psi_{\text{EP},2}$ with $dN^{J/\psi}/d\Delta\varphi = A \times (1 + 2v_2^{\text{obs}} \cos 2\Delta\varphi)$, where
 26 A is a normalization constant (the standard event plane method), as shown in Fig. 1 (left panel).
 27 At LHC, the event-plane-resolution-corrected v_2 of J/ψ with $2 < p_T < 4$ GeV/ c is different from
 28 the STAR preliminary measurement which is compatible with zero in all the measured p_T range,
 29 as shown in Fig. 1 (right panel). Two model calculations based on transport mechanism which
 30 include a J/ψ regeneration component from deconfined charm quarks in the medium [10, 11]
 31 are compared with data. These two models differ mostly in the rate equation controlling the J/ψ
 32 dissociation and regeneration. In both models about 50% of the produced J/ψ mesons originate
 33 from regeneration in QGP in the most central collisions. On one hand, thermalized charm quarks
 34 in the medium will transfer a significant elliptic flow to regenerated J/ψ . The maximum v_2 at
 35 $p_T \approx 2.5$ GeV/ c results from a dominant contribution of regeneration at lower p_T with respect to
 36 the initial J/ψ component. Both models are able to qualitatively describe J/ψ $v_2(p_T)$ data as both
 37 were also able to describe the earlier R_{AA} measurement [2].

38 Consistent results in the same centrality bin are obtained with an invariant mass fit technique,
 39 in which we fit the $v_2 = \langle \cos 2\Delta\varphi \rangle$ vs. invariant mass ($m_{\mu\mu}$) as described in [12]. The method
 40 involves calculating the v_2 of the OS dimuons as a function of $m_{\mu\mu}$ and then fitting the resulting
 41 $v_2(m_{\mu\mu})$ distribution using: $v_2(m_{\mu\mu}) = v_2^{\text{sig}} \alpha(m_{\mu\mu}) + v_2^{\text{bkg}}(m_{\mu\mu})[1 - \alpha(m_{\mu\mu})]$, where v_2^{sig} is the J/ψ
 42 elliptic flow and v_2^{bkg} is the background flow (parametrized using a second order polynomial
 43 function in this analysis). $\alpha(m_{\mu\mu}) = S/(S + B)$ is the ratio of the signal over the sum of the
 44 signal plus background of the $m_{\mu\mu}$ distributions. $\alpha(m_{\mu\mu})$ is extracted from fits to the OS invariant
 45 mass distribution in each p_T and centrality class. The OS dimuon invariant mass distribution
 46 was fitted with a Crystal Ball (CB) function to reproduce the J/ψ line shape, and either a third
 47 order polynomial or a variable width gaussian to describe the underlying continuum. The CB
 48 function connects a Gaussian core with a power-law tail [13] at low mass to account for energy

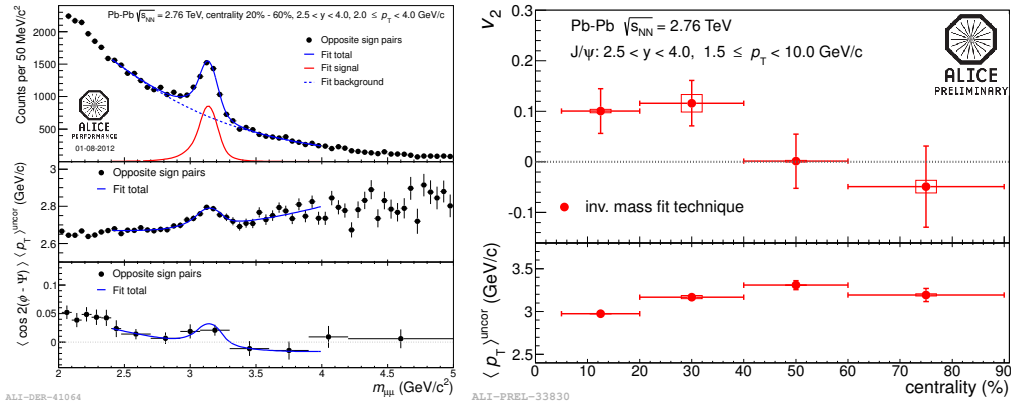


Figure 2: Left: $\langle p_T \rangle^{\text{uncor}}$ and v_2 extraction with the fit invariant mass technique. Right: Event plane resolution corrected J/ψ v_2 as a function of centrality of J/ψ with $p_T \geq 1.5$ GeV/c. The vertical bars show the statistical uncertainties, and the boxes indicate the point-to-point uncorrelated systematic uncertainties, which are dominated by the signal extraction.

49 loss fluctuations and radiative decays. The combination of several CB and underlying continuum
50 parametrization were tested to assess the signal and the related systematic uncertainties. The J/ψ
51 v_2 in each p_T and centrality class was determined as the average of the v_2^{sig} obtained by fitting
52 $v_2(m_{\mu\mu})$ with various background shapes, while the corresponding systematic uncertainties were
53 defined as the *r.m.s.* of these results. A similar method is used to extract the uncorrected average
54 transverse momentum $\langle p_T \rangle^{\text{uncor}}$ of the reconstructed J/ψ in each centrality and p_T class. Fig. 2
55 (left panel) shows typical fits of the OS invariant mass distribution (top left), the $\langle \cos 2(\phi - \Psi_{EP,2}) \rangle$
56 (bottom left) and $\langle p_T \rangle^{\text{uncor}}$ (middle left) as a function of $m_{\mu\mu}$ in the 20%-60% centrality class. The
57 obtained J/ψ $\langle p_T \rangle^{\text{uncor}}$ is used to locate the ALICE points when plotted as a function of transverse
58 momentum.

59 Fig. 2 (top right) shows v_2 for inclusive J/ψ with $p_T \geq 1.5$ GeV/c as a function of centrality.
60 The vertical bars show the statistical uncertainties while the boxes indicate the point-to-point
61 uncorrelated systematic uncertainties from the signal extraction. The measured v_2 depends on
62 the p_T distribution of the reconstructed J/ψ . Therefore, $\langle p_T \rangle^{\text{uncor}}$ of the reconstructed v_2 is also
63 shown in Fig. 2 (bottom right) as a function of centrality. For the two most central bins, 5%-20%
64 and 20%-40% the inclusive J/ψ v_2 for $p_T \geq 1.5$ GeV/c are $0.101 \pm 0.044(\text{stat.}) \pm 0.003(\text{syst.})$
65 and $0.116 \pm 0.045(\text{stat.}) \pm 0.017(\text{syst.})$, respectively. For the two most peripheral bins the v_2 is
66 consistent with zero within uncertainties. Although there is a small variation with centrality, the
67 $\langle p_T \rangle^{\text{uncor}}$ stays in the range (3.0, 3.3) GeV/c indicating that the bulk of the reconstructed J/ψ are
68 in the same intermediate p_T range for all centralities. Thus, the observed centrality dependence
69 of the v_2 for inclusive J/ψ with $p_T \geq 1.5$ GeV/c does not result from any bias in the sampled p_T
70 distributions.

71 Fig. 3 shows the inclusive J/ψ $v_2(p_T)$, using the invariant mass fit technique, for central, semi-
72 central and peripheral Pb-Pb collisions at 2.76 TeV. In the semi-central (20%-40%) case, taking
73 into account statistical and systematic uncertainties, the combined significance of a non-zero v_2
74 in $2 \leq p_T < 6$ GeV/c range is 3σ . At lower and higher transverse momentum the inclusive
75 J/ψ v_2 is compatible with zero within uncertainties. In most central (5%-20%) and peripheral
76 (40%-60%) case, the large uncertainties do not allow any firm conclusion.

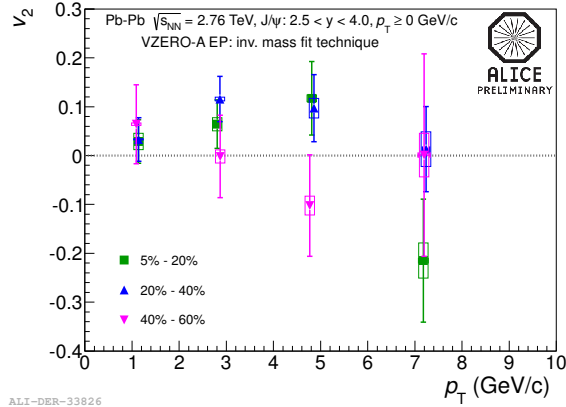


Figure 3: J/ψ v_2 as a function of p_T in various centrality bins: 5%-20%, 20%-40% and 40%-60%. The vertical bars show the statistical uncertainties, and the boxes indicate the point-to-point uncorrelated systematic uncertainties from the signal extraction.

77 3. Summary and conclusion

78 In summary, we reported the ALICE measurement of inclusive J/ψ v_2 at forward rapidity in
 79 Pb-Pb collisions at $\sqrt{s_{NN}} = 2.76$ TeV. For non-central (20%-60%) collisions a hint of a non-zero
 80 J/ψ elliptic flow is observed in the intermediate p_T range in contrast to the zero v_2 observed at
 81 RHIC. Indication of a non-zero J/ψ v_2 is also observed in semi-central (20%-40%) collisions at
 82 intermediate p_T . The integrated v_2 of J/ψ with $p_T > 1.5$ GeV/c in 5%-40% collisions also shows
 83 a non-zero behavior. These measurements complement our earlier results on J/ψ suppression,
 84 where a smaller suppression was seen at low transverse momentum at the LHC compared to
 85 RHIC [2, 7, 14]. Both results taken together could indicate that a significant fraction of the
 86 observed J/ψ are produced from a (re)combination of the initially produced charm quarks. Our
 87 J/ψ elliptic flow results in Pb-Pb collisions at $\sqrt{s_{NN}} = 2.76$ TeV are in qualitative agreement with
 88 transport models that are able to reproduce our J/ψ R_{AA} measurement.

89 References

- 90 [1] T. Matsui and H. Satz, Phys. Lett., B178, p. 416, 1986.
 91 [2] B. Abelev *et al.* [ALICE Collaboration] Phys. Rev. Lett. 109, 072301, 2012.
 92 [3] B. Alessandro *et al.*, Eur. Phys. J., C39, p. 335–345, 2005.
 93 [4] A. Adare *et al.*, Phys. Rev. Lett., 98, p. 232301, 2007; Phys. Rev., C84, p. 054912, 2011.
 94 [5] Z. Tang [STAR collaboration], J. Phys. G38, 12417, 2011.
 95 [6] K. Aamodt *et al.*, [ALICE Collaboration], JINST 3, S08002, 2008.
 96 [7] R. Arnardi, these proceedings.
 97 [8] A. M. Poskanzer and S. A. Voloshin Phys. Rev. C 58, 1671, 1998.
 98 [9] L. Massacrier, Hard Probes 2012 proceedings arXiv:1208.5401, and references therein.
 99 [10] Y.-P. Liu, *et al.*, Phys. Lett. B678, pp. 72–76, 2009 and priv. comm. in 2012.
 100 [11] X. Zhao and R. Rapp, Nucl. Phys., A 859, pp. 114–125, 2011, R. Rapp these proceedings, and priv. comm. in 2012.
 101 [12] N. Borghini and J. Ollitrault, Phys. Rev. C70, 064905, 2004, arXiv:nucl-th/0407041 [nucl-th].
 102 [13] J. E. Gaiser, Ph.D. thesis, Stanford (1982), appendix-F, SLAC-R-255.
 103 [14] E. Scomparin, these proceedings.